

# Simultaneous CAR- and $\alpha_v$ Integrin-Binding Ablation Fails to Reduce Ad5 Liver Tropism

Karine Martin,<sup>1</sup> Anne Brie,<sup>1,\*</sup> Patrick Saulnier,<sup>2</sup> Michel Perricaudet,<sup>1</sup>  
Patrice Yeh,<sup>1,\*</sup> and Emmanuelle Vigne<sup>1,\*†</sup>

<sup>1</sup>UMR1582 CNRS/IGR/Aventis-Gencell and <sup>2</sup>Centre de Référence, IGR/Aventis-Gencell, Institut Gustave Roussy, 94805 Villejuif Cedex, France

\*Present address: Gencell S.A.S., 94403 Vitry-sur-Seine, France.

†To whom correspondence and reprint requests should be addressed at Gencell S.A.S., CRVA, 13 Quai Jules Guedes, 94403 Vitry-sur-Seine, France.  
Fax: 33 1 58 93 24 22. E-mail: emmanuelle.vigne@gencell.com.

Targeting adenovirus encoding therapeutic genes to specific cell types has become a major goal in gene therapy. Coxsackievirus and adenovirus receptor (CAR) and  $\alpha_v$  integrins have been identified as the primary cell surface components that interact with adenovirus type 5 (Ad5)-based vectors during *in vitro* transduction. Redirecting Ad5-based vectors requires abrogation of the natural interaction between the viral capsid and its cellular receptors and simultaneous introduction of a new binding specificity into the viral capsid. To abrogate native Ad5 tropism, fiber knob mutations Pro409Glu and Lys417Ala were each incorporated into adenoviral vectors, while the RGD motif was deleted from the penton base. *In vitro* transduction experiments showed that these capsid mutations eliminated Ad5 interactions with CAR and  $\alpha_v$  integrins. Moreover, incorporation in the fiber HI loop of a vitronectin-derived ligand (VN4) specific for the uPAR/CD87 receptor provided the Lys417Ala virus with an alternative entry pathway specific for uPAR-expressing cells, indicating a successful *in vitro* retargeting of the vector. Unexpectedly, however, simultaneous disruption of Ad5 binding to CAR and  $\alpha_v$  integrins had no effect on liver gene transfer following systemic administration in mice. This study highlights the need to understand better the molecular determinants involved in adenovirus uptake by the liver to control the fate of adenoviral vectors *in vivo*.

**Key Words:** adenovirus vector, targeting, fiber, CAR,  $\alpha_v$  integrins, tropism

## INTRODUCTION

Controlling adenovirus (Ad) tropism has become a major challenge to enhance the therapeutic potential of adenovectors, particularly in cancer gene therapy. Indeed, intravascular application of antitumor vectors is a prerequisite to reach all metastases and a maximum of tumor cells within tumors. To this end, Ad vector tropism should be restricted specifically to proliferating/migrating cells from the tumor and/or tumor endothelium, thereby reducing the undesired interactions between virus and non-target tissues and minimizing possible toxicities and host immune responses [1]. The urokinase-type plasminogen activator receptor (uPAR/CD87) is an attractive candidate as target receptor to mediate gene delivery to these cells. uPAR is a multifunctional cell surface receptor that is critically involved in cellular adhesion, migration and invasion, and signaling [for review, see 2]. The expression

level of uPAR on cells strongly correlates with their migratory and invasive potential. Upregulation of uPAR constitutes a poor prognosis marker for a variety of metastatic cancers, including breast, prostate, and colon carcinomas [3]. uPAR expression has also been identified in the angiogenic vasculature of solid tumors, such as colon and breast carcinomas [4,5].

Adenovirus type 5 (Ad5) attachment to the cell surface is mediated through a high-affinity interaction between the C-terminal knob of the viral fiber protein and the cellular CAR protein (coxsackievirus and adenovirus receptor) [6,7]. In a second step, an interaction between the RGD motif of the viral penton base protein with cellular  $\alpha_v$  integrins facilitates internalization of the virus [8–10]. A direct correlation between CAR expression level and efficiency of adenovirus-mediated gene transfer has been reported in a large number of cell types *in vitro* [11–14]. In particular, the poor susceptibility of many primary tu-

**TABLE 1:** Description and physical characteristics of capsid-modified viruses

Virus	Fiber mutation <sup>a</sup>	Penton base mutation	Targeting ligand	VP <sup>b</sup> /ml
Ad-CTL	—	—	—	$6.77 \times 10^{12}$
Ad-VN4	—	—	VN4	$2.60 \times 10^{12}$
Ad-PB <sub>μ</sub>	—	ΔRGD	—	$2.20 \times 10^{12}$
Ad-P409E	P409E (AB loop)	—	—	$1.24 \times 10^{13}$
Ad-K417A	K417A (AB loop)	—	—	$8.32 \times 10^{11}$
Ad-ΔTAYT	ΔTAYT(489–492)	—	—	$4.59 \times 10^{12}$
Ad-K417A-VN4	K417A (AB loop)	—	VN4	$1.36 \times 10^{12}$
Ad-K417A-PB <sub>μ</sub>	K417A (AB loop)	ΔRGD	—	$5.79 \times 10^{12}$
Ad-K417A-VN4-PB <sub>μ</sub>	K417A (AB loop)	ΔRGD	VN4	$1.79 \times 10^{12}$

<sup>a</sup>Amino acid residues are numbered according to the system of Xia *et al.* [44].

<sup>b</sup>VP, viral particle titers as determined by HPLC [43].

mors [15,16] to adenovectors is essentially due to low CAR expression. The interaction of fiber knob with CAR has been well characterized. The crystal structure of the Ad12 knob in complex with the N-terminal portion of CAR demonstrated that part of the AB, DE, and FG loops as well as the very short F strand of fiber knob are key players in the binding with CAR [17]. Consistently, it was shown that mutagenesis of various residues in these target regions of Ad5 fiber eliminated high-affinity binding to human CAR, eventually resulting in a dramatic decrease in CAR-positive cell transduction *in vitro* [18–27].

The contribution of CAR to *in vivo* gene transfer remains, however, unclear. Although high levels of CAR expression are observed in several mice organs, liver is by far the major tissue transduced following Ad5 intravenous administration [28,29]. Until recently, it was accepted that CAR interaction was the major determinant of hepatocyte transduction *in vivo* and that eliminating knob binding to CAR would result in the loss of Ad5 hepatotropism. Unexpectedly, fiber mutations that abolish interaction with CAR were reported to be not sufficient to impair liver gene transfer following intravenous injection in mice [21,24,25,27], showing that other pathways are likely involved in the uptake of adenoviral vectors by liver. In particular, Einfeld *et al.* have reported that the disruption of both CAR and  $\alpha_v$  integrin interactions may be critical for effectively reducing Ad5 native tropism [26].

In this study, we investigated the possibility of developing Ad5 vectors genetically engineered to specifically target the uPAR/CD87. We combined capsid mutations designed to ablate CAR and  $\alpha_v$  integrin binding, with the insertion in the fiber knob of a vitronectin peptide displaying high affinity for uPAR. This study reports the *in vitro* and *in vivo* transduction properties of the capsid-modified vectors.

## RESULTS

### Construction of Capsid-Modified Viruses

The crystal structure of the Ad12 fiber knob in complex with domain I of CAR [17] has revealed the key residues involved in the Ad12 knob–CAR interface, in particular AB loop proline 418 and aspartate 415, leucine 426, and lysine 429. Abrogating the interactions between CAR and P418 or L426 resulted in the complete elimination of the binding of the Ad12 knob to CAR [17]. Based on the structural superimposition of the very similar Ad12 and Ad5 knob, we hypothesized that the Ad5 residues P409 and K417 should play in the interaction between Ad5 knob and CAR the same critical role as Ad12 P418 and L426, respectively. Accordingly, we constructed the two fiber-mutated vectors Ad-P409E and Ad-K417A by incorporating the P409E and K417A mutations into the fiber knob of the control Ad-CTL vector (Table 1). As a control, we generated Ad-ΔTAYT, the fiber of which carries a deletion previously shown to diminish fiber-dependent adenoviral gene transfer [18]. We further modified the viral capsid of control Ad-CTL and mutant Ad-K417A by deleting the RGD motif from their penton base (Table 1). To retarget the vector to the uPAR receptor, we inserted the 12-amino-acid VN4 peptide into the HI fiber loop of control Ad-CTL and mutant Ad-K417A or Ad-K417A-PB<sub>μ</sub> (Table 1). All vectors express the nuclear  $\beta$ -galactosidase from the human cytomegalovirus promoter/enhancer. All viruses were viable, and if suitable infection conditions were provided (see Materials and Methods for details), expansion of the vectors in production runs showed comparable yields for the modified and control vectors (Table 1).

We analyzed viral purified preparations by Western blotting using antibodies directed against the fiber or the whole Ad5 capsid (not shown). This evidenced that the protein profiles of all viruses were comparable to that of

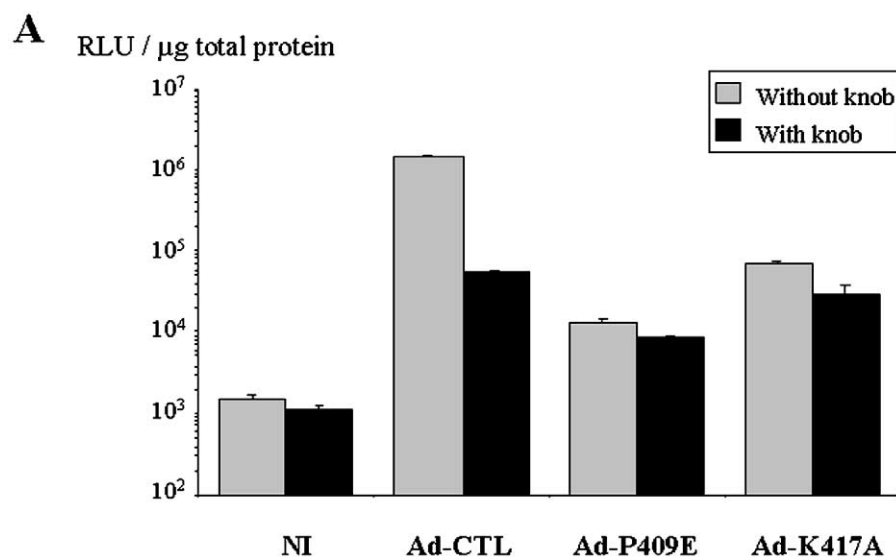
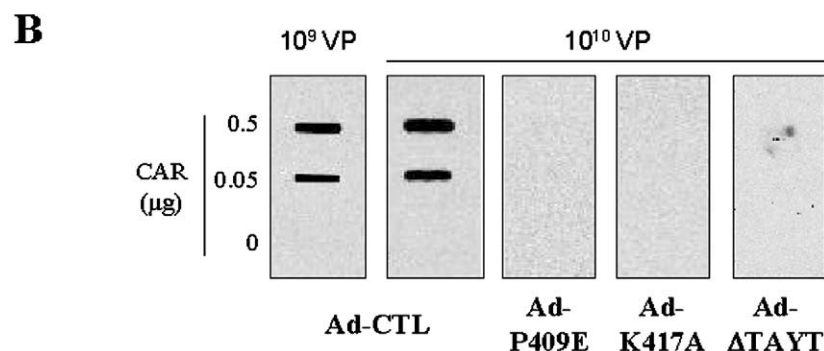


**FIG. 1.** *In vitro* CAR binding of fiber-modified viruses. (A) Competition experiment with soluble knob in 293 cells. Confluent monolayers of 293 were preincubated in the absence or presence of 10  $\mu\text{g}/\text{ml}$  Ad5 knob protein for 30 min at room temperature. Each virus was then added to the cells at an m.o.i. of 50 VP/cell and incubated for 30 min at room temperature. Cells were washed twice with PBS and incubated for 24 h at 37°C in MEM-10% FBS.  $\beta$ -Galactosidase activity was measured in a chemiluminescence assay. (B) *In vitro* binding of fiber-modified viruses to soluble CAR. Soluble CAR was immobilized on nitrocellulose membranes. Membranes were blocked in PBS-5% nonfat milk and then incubated overnight at 4°C with  $10^9$  or  $10^{10}$  VP of virus. Detection was performed as described under Materials and Methods.



control vector Ad-CTL and that all viruses incorporated the modified fiber proteins in stoichiometric amounts in the viral capsid. Furthermore, the precursors of the viral pVI, pVII, and pVIII proteins were not detected, indicating a normal proteolytic processing. That the HPLC profiles of modified capsids (not shown) were unchanged compared to Ad-CTL suggests that fiber mutations did not critically interfere with capsid assembly and maturation steps necessary to allow subsequent effective entry into cells. Finally, we confirmed by electron microscopy (not shown) that viral particles of all mutant viruses were similar in aspect to those of the control virus (no abnormal aggregation or degradation).

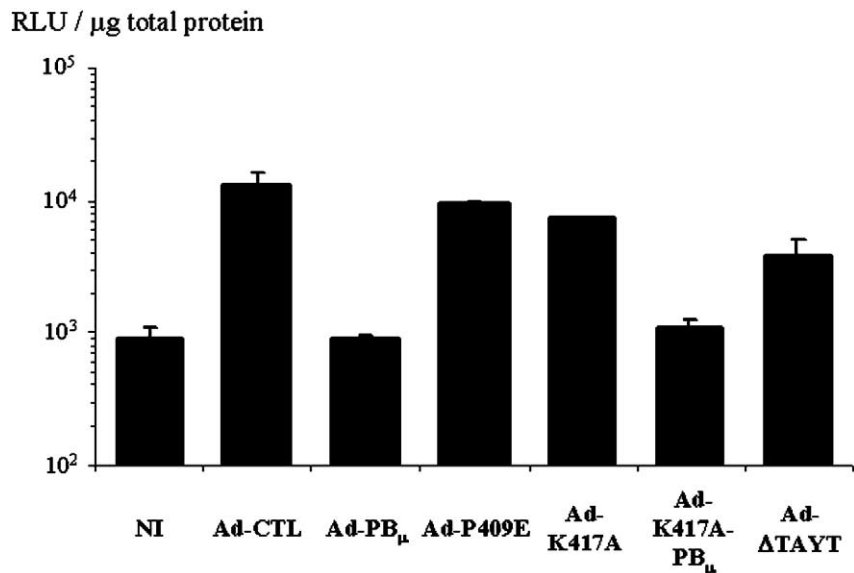
#### *In Vitro* Characterization of the Mutant Viruses

We first investigated the impact of the fiber knob mutations on the efficiency of gene transfer into the CAR- and  $\alpha_v$ -integrin-positive 293 cells.  $\beta$ -Galactosidase activity fol-

lowing infection of these cells with Ad-P409E, Ad-K417A, and Ad- $\Delta$ TAYT mutants was 20- to 100-fold lower than with the control virus Ad-CTL (Fig. 1A and data not shown). Moreover, infection was not inhibited by preincubation with a saturating concentration of soluble knob (Fig. 1A), suggesting that knob did not mediate viral attachment to the cell and that the corresponding mutations P409E, K417A, and  $\Delta$ TAYT had a significant effect on CAR binding. To study directly the interaction between the modified viruses and CAR, we immobilized soluble CAR on nitrocellulose membranes and tested it for its ability to bind to the different viruses (Fig. 1B). As expected, the three fiber-mutated viruses were no longer able to bind to soluble CAR.

To evaluate the influence of the RGD motif deletion from Ad-CTL and Ad-K417A penton base on binding to  $\alpha_v$  integrins, we infected the CAR-negative/ $\alpha_v$  integrin-

**FIG. 2.** CAR-negative/ $\alpha_v$  integrin-positive cell transduction with capsid-modified viruses. Modified and control viruses were incubated with L929 cells at an m.o.i. of 10,000 VP/cell for 48 h at 37°C before  $\beta$ -galactosidase activity was measured in a chemiluminescence assay.



positive L929 cells [30] using conditions allowing significant gene transfer with the control vector Ad-CTL (multiplicity of infection (m.o.i.) 10,000 viral particles (VP)/cell and 48 h incubation of the virus onto cells). As expected, both RGD-deleted viruses Ad-PB<sub>μ</sub> and Ad-K417A-PB<sub>μ</sub> were unable to transduce L929 cells (Fig. 2). In addition, Ad-P409E, Ad-K417A, and Ad- $\Delta$ TAYT were capable of transducing these CAR-negative cells as efficiently as Ad-CTL, indicating that the P409E, K417A, and  $\Delta$ TAYT fiber mutations did not affect any characteristics of the virion required to allow efficient intracellular trafficking following internalization.

#### Incorporation of a Targeting Ligand

We next investigated the feasibility of retargeting the Ad5 virion to the uPAR. We had previously demonstrated that the Ad-VN4 vector (Table 1), of which the HI loop of the knob is substituted with VN4, a high-affinity ligand for uPAR derived from human vitronectin, transduces uPAR-positive cells in a CAR-independent manner (E. Vigne, manuscript in preparation). Therefore, the VN4 peptide was introduced into viruses Ad-K417A and Ad-K417A-PB<sub>μ</sub> to generate mutant viruses Ad-K417A-VN4 and Ad-K417A-VN4-PB<sub>μ</sub>. We first compared the transduction properties of these viruses in the uPAR-positive 293 cells. Fig. 3A shows that vectors Ad-VN4 and Ad-K417A-VN4, which display the VN4 peptide in an otherwise wild-type or K417A-mutated fiber knob, transduce these uPAR-positive cells with equally high efficiency. Furthermore, while transduction with Ad-CTL was inhibited by addition of soluble knob, this had little to no effect on infection with both VN4-containing vectors, providing further evidence that VN4 could mediate cell entry in a CAR-independent way. In addition, we showed that Ad-K417A-

VN4 was unable to bind to immobilized soluble CAR (data not shown), indicating that the VN4 insertion in Ad-K417A did not restore binding to CAR by altering the knob structure. Infection of uPAR-positive L929 cells confirmed that the VN4 insertion provides the Ad5 virion with an efficient CAR-independent entry pathway. In addition, this demonstrated that the RGD deletion from the Ad-K417A-VN4 capsid had a minor impact on cell transduction (Fig. 3B). Altogether, these results demonstrated that the inclusion of the VN4 peptide in the fiber knob of a CAR- and integrin-binding ablated vector allows efficient retargeting of the adenoviral vector to an alternative cell-surface receptor.

In general, strong uPAR expression is observed in organs undergoing extensive tissue remodeling and in migrating cells. Accordingly, uPAR has been shown to be absent from quiescent hepatocytes [28]. We evaluated the permissivity of rat primary hepatocytes, known to be CAR- and  $\alpha_v$  integrin-positive [31], to the VN4-displaying viruses. As expected, the CAR-binding-ablated Ad-K417A was ineffective in transducing these cells (Fig. 4) and Ad-K417A-VN4 reporter gene expression was not different from that of Ad-K417A. This result provided further evidence that the VN4 inclusion did not restore binding to CAR. Most importantly, this demonstrated that the VN4 insertion did not confer to the retargeted vectors an entry pathway suitable for the uPAR-negative hepatocytes.

#### *In Vivo* Characterization of the Capsid-Modified Viruses after Systemic Delivery

Intravenous administration of Ad5-based vectors in mice results in preferential transgene expression in the liver, which is the prominent organ for CAR expression. To compare the liver tropism of our mutant viruses, we in-

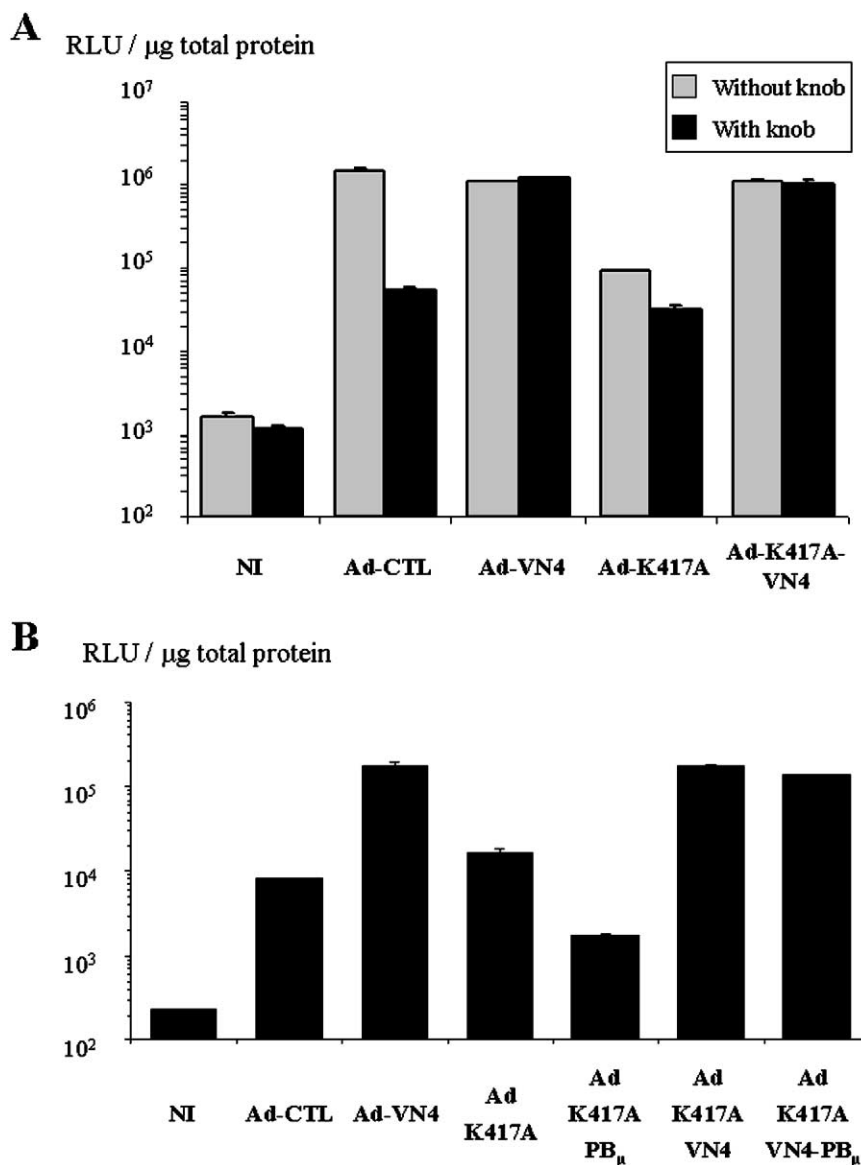


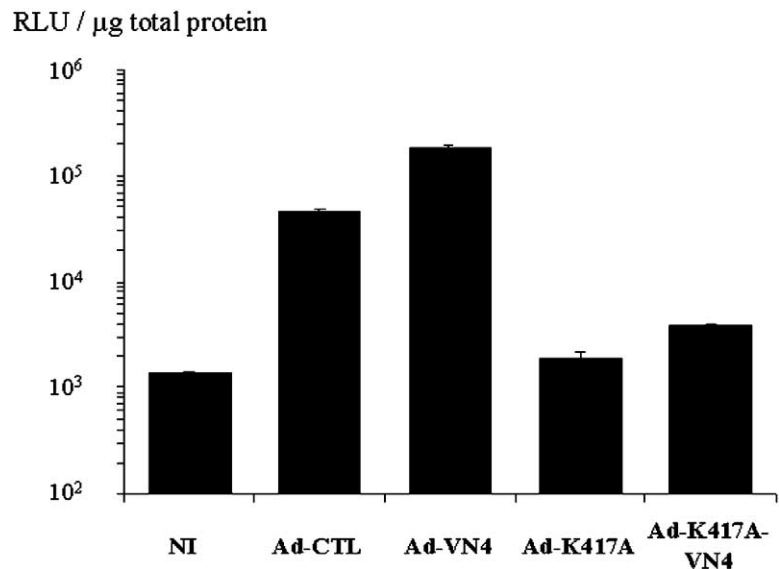
**FIG. 3.** *In vitro* retargeting of Ad5 to uPAR-positive cells. (A) Competition experiment with soluble knob in 293 cells. Confluent monolayers of 293 cells (CAR<sup>+</sup>,  $\alpha_v$  integrin<sup>+</sup>, uPAR<sup>+</sup>) were preincubated in the presence or absence of 10  $\mu\text{g}/\text{ml}$  Ad5 knob protein for 30 min at room temperature. Each virus was then added to the cells at an m.o.i. of 50 VP/cell and incubated for 30 min at room temperature. Cells were washed twice with PBS and incubated for 24 h at 37°C in MEM-10% FBS.  $\beta$ -Galactosidase activity was measured in a chemiluminescence assay. (B) Transduction efficiency of capsid-modified viruses in L929 cells. Viruses were incubated on L929 cells (CAR<sup>-</sup>,  $\alpha_v$  integrin<sup>+</sup>, uPAR<sup>+</sup>) at an m.o.i. of 10,000 VP/cell for 24 h at 37°C before  $\beta$ -galactosidase activity was measured in a chemiluminescence assay.

jected C57BL/6 mice intravenously with  $3 \times 10^{10}$  VP of viruses. We assessed the liver transduction efficiency by determining  $\beta$ -galactosidase expression and vector DNA content 2 days postinjection. Fig. 5 shows no significant difference in  $\beta$ -galactosidase activity between the CAR-binding-ablated Ad-K417A and Ad-P409E vectors and the control Ad-CTL. We obtained similar results with Ad- $\Delta$ TAYT (not shown), indicating that CAR-binding ablation through P409E and K417A knob mutations or  $\Delta$ TAYT deletion did not modify Ad5 liver tropism. Most interestingly, mutant Ad-K417A-PB $_{\mu}$ , whose interactions with both CAR and  $\alpha_v$  integrins were abolished by simultaneous K417A knob mutation and deletion of the RGD motif from the penton base, transduced liver as well as the

control vector Ad-CTL (Fig. 5). Importantly, the VN4 insertion in the HI loop of Ad-CTL, Ad-K417A, or Ad-K417A-PB $_{\mu}$  virus did not influence liver gene transfer either (not shown). Using real-time PCR, we found a similar number of relative vector copies for each vector in the liver, thus confirming the gene expression results (Table 2 and data not shown). Immunohistochemical staining for  $\beta$ -galactosidase confirmed the results of the enzymatic activity assay and the PCR analysis (data not shown), showing that all vectors transduced hepatocytes equally well.

We analyzed additional tissues from these mice for  $\beta$ -galactosidase expression to examine the vector distribution. The level of transduction detected with Ad-CTL in

**FIG. 4.** Transduction efficiency of capsid-modified viruses in rat primary hepatocytes. Rat primary hepatocytes were incubated with the control or capsid-modified viruses or medium alone (NI) at an m.o.i. of 100 VP/cell for 30 min at 37°C. Cells were washed twice with PBS and further incubated with fresh medium at 37°C for 24 h.  $\beta$ -Galactosidase activity was measured using a chemiluminescence reporter assay.



spleen, lung, heart, and kidney was  $\leq 0.2\%$  of that found in the liver and most often not significantly above the background (Fig. 5). Consequently, we used real-time Taqman PCR analysis to quantify the vector distribution more accurately. Importantly, Taqman PCR allowed the detection of significant amounts of vector DNA in all organs. We found that CAR-binding ablation alone had no significant effect on the level of vector genomes in any of the tissues tested (Table 2). In contrast, Ad-K417A-PB<sub>μ</sub> levels were significantly reduced relative to Ad-K417A levels in the heart ( $P < 0.03$ ), lung ( $P < 0.01$ ), and kidney ( $P < 0.02$ ). Taken together, these results indicate an absence of effect on liver transduction of the fiber and penton base modifications and an alteration of the distribution to other organs following the concomitant loss of CAR and integrin binding.

## DISCUSSION

In this study, we endeavored to retarget Ad5-based vectors by simultaneous removal of CAR and  $\alpha_v$  integrin binding

and appending a new entry pathway. Structural analysis [17] has initially revealed that human CAR binds the Ad12 fiber knob at the interface between two adjacent knob monomers, specifically the AB loop, the DE loop, and the F strand of one monomer and the FG loop of the adjacent monomer. Surface plasmon resonance and competition experiments based on mutants of the Ad5 fiber knob domain further confirmed that the CAR-binding site of the Ad5 fiber knob consists of part of the AB and DG loops and of the B, E, and F  $\beta$  strands [18,19,32]. To ablate Ad5 binding to CAR and/or  $\alpha_v$  integrins, we generated vectors whose fiber knob residue P409 or K417 was mutated and/or whose penton base was deleted from its RGD motif (Table 1). Using optimized conditions, all viruses could be grown in a standard E1-transcomplementing cell line without complementing for the fiber or providing an alternative binding between the virus and the packaging cells. A systematic control evidenced that the quality of the purified viral batches was the same for all viruses, so that the differences of transduction features could not be ascribed to a variable quality of preparations.

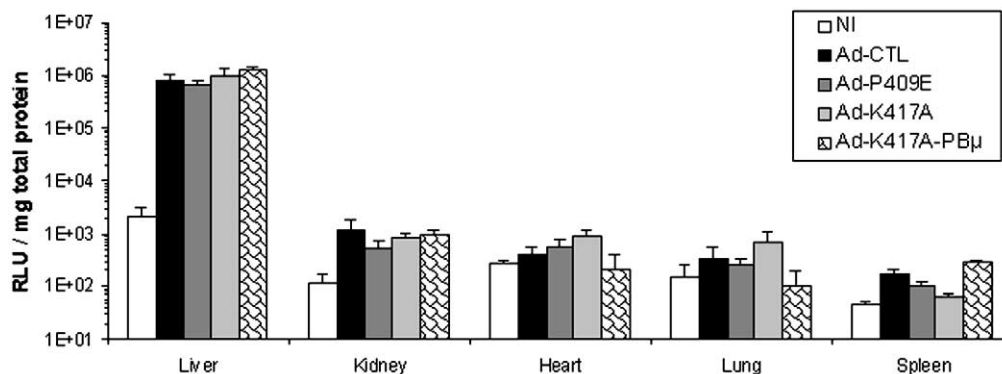


**FIG. 5.** *In vivo* characterization of capsid-modified viruses after systemic delivery. C57BL/6 mice were injected with buffer (NI) or  $3 \times 10^{10}$  VP of control or modified viruses. Animals were sacrificed at day 2 following injection. Liver, heart, lung, kidney, and spleen were collected 48 h postinjection. The average  $\beta$ -galactosidase activity level normalized to the protein content of the samples  $\pm$  SEM is shown for each treatment group ( $n = 10$  per group).

**TABLE 2:** *In vivo* adenoviral vector biodistribution as analyzed by Taqman PCR<sup>a</sup>

Tissue	Relative number of viral genome copies (% of Ad-CTL value) <sup>b</sup>		
	Ad-CTL	Ad-K417A	Ad-K417A-PB <sub>μ</sub>
Liver	100 ± 13	74.1 ± 23	89.1 ± 23
Spleen	100 ± 26	172.6 ± 17	53.5 ± 3.8
Lung	100 ± 65	109.6 ± 16	3.9 ± 1.1*
Heart	100 ± 23	254.4 ± 148	7.2 ± 4*
Kidney	100 ± 26	157.3 ± 36	11.4 ± 7.2*

<sup>a</sup>Results were obtained as the number of copies per microgram of genomic DNA.

<sup>b</sup>Results are reported as percentage of the number of copies of Ad-CTL detected in each tissue. The values are expressed as mean ± SEM, *n* = 5 mice per group.

\*Significant difference with Ad-K417A (*P* < 0.03).

The *in vitro* characterization of the mutant viruses revealed the dramatic impact of the AB loop mutations P409E and K417A on CAR binding and subsequent gene transfer efficiency. Indeed, viruses Ad-P409E and Ad-K417A exhibited a significant reduction in the transduction efficiency for CAR-positive cells such as 293 cells (Fig. 1A) or primary rat hepatocytes (Fig. 4). The low-level transduction observed was not inhibited by recombinant Ad5 knob in 293 cells (Fig. 1A), providing further evidence that these viruses have no residual CAR-binding activity. This was also evidenced by the absence of detectable binding of these viruses to immobilized soluble CAR (Fig. 1B). The effect of P409E and K417A knob mutations is in agreement with previous reports showing that binding to soluble CAR of recombinant Ad5 knob displaying P409A or K417G mutations is abrogated [18] and that the Ad5 knob P409 is a contact residue with CAR [32]. To disable the Ad5 cell entry pathway further, the K417A fiber mutation was combined with the deletion of the RGD penton base motif, thereby preventing the virus from interacting with cellular  $\alpha_v$  integrins. The impact of the RGD deletion from wild-type or K417A capsids was dramatic in the CAR-negative/ $\alpha_v$  integrin-positive L929 cells, in which gene transfer with both the RGD-deleted Ad-PB<sub>μ</sub> and the doubly ablated Ad-K417A-PB<sub>μ</sub> vectors was virtually abolished (Fig. 2). Importantly, the three CAR-binding-ablated Ad-P409E, Ad-K417A, and Ad- $\Delta$ TAYT vectors transduced these cells as efficiently as the control vector, indicating that P409A, K417A, and  $\Delta$ TAYT fiber mutations had no impact on any intracellular trafficking steps following virion internalization.

The development of retargeted vectors relies on the identification and validation of targeting ligands. In another study (E. Vigne, manuscript in preparation), we have shown that VN4, a 12-amino-acid peptide of the human vitronectin displaying a strong affinity for the uPAR [33], can provide Ad5-based vectors with an alternative entry pathway when incorporated within the knob

HI loop. uPAR is an attractive target for mediating binding of engineered adenoviral vectors. Indeed, it is known to be critically involved in cellular adhesion, migration, and invasion and has been widely reported to be overexpressed in migrating cells such as vascular smooth muscle cells, tumor cells (from both primary bed and metastases), and activated endothelium [2]. Here, we showed that the VN4 peptide could provide to the Ad-K417A and Ad-K417A-PB<sub>μ</sub> vectors a very efficient CAR-independent entry pathway in uPAR-positive cell lines (Fig. 3B). Moreover, we demonstrated that VN4 inclusion in the HI loop did not alter the knob structure in such a way that it could rescue the CAR-binding deficiency. Most importantly, we showed that the VN4 peptide did not provide an entry pathway suitable for hepatocyte infection (Fig. 4), setting up the VN4-displaying CAR- and  $\alpha_v$  integrin-binding-ablated vectors as good candidates for *in vivo* retargeting to uPAR-positive tissues.

Several groups have identified fiber knob mutations that successfully ablate the virus-CAR interaction *in vitro*. Indeed, substitutions in the AB loop (S408E [21], S408E-P409G [24], R<sub>412</sub>AEK<sub>417</sub> → SGGG [26]) and in the DE loop (Y477A [27]), and to a lesser extent in the CD loop (V441A-K442A [20]), as well as mutations in the FG loop (deletion of T<sub>489</sub>AYT<sub>492</sub> [18], Y491D, A494D, or A503D [21]), induce a dramatic reduction in transduction of various CAR-positive cell lines. However, the contribution of CAR to *in vivo* gene transfer to the liver is much less clear. All published studies except that of Einfeld *et al.* [26] have shown that eliminating CAR binding through discrete knob mutation does not alter *in vivo* distribution following systemic delivery in the mice [21,24,25,27]. In the present study, we also report no significant reduction in liver transduction with the CAR-binding-ablated viruses displaying mutations P409A, K417A, or  $\Delta$ TAYT (Fig. 5 and Table 2 and data not shown). That these CAR-binding-ablated viruses were unable to transduce primary rat hepatocytes *in vitro* (Fig. 4 and data not shown) provides further evidence that *in vivo* hepatic gene transfer occurs mainly in a CAR-independent manner. Einfeld *et al.* have reported a dramatic drop in liver transduction with a virus disabled in both CAR and  $\alpha_v$  integrin interactions [26]. In contrast, we observed that the Ad-K417A-PB<sub>μ</sub> vector, which combines the K417A CAR-ablating mutation and the deletion of the penton base RGD motif, transduces liver cells as well as the control vector (Fig. 5 and Table 2), demonstrating that the concomitant disruption of binding to CAR and  $\alpha_v$  integrin is not sufficient to abolish liver tropism *in vivo*. In addition, we did not observe any effect of the sole deletion of the RGD motif from penton base (Ad-PB<sub>μ</sub>) on liver gene transfer (data not shown). Most importantly, that the VN4 insertion in the HI loop of our capsid mutant vectors had no impact on gene transfer to the liver provided evidence that this peptide does not direct the vector to unexpected target in healthy animals.

In agreement with published data [21,24,26,27], the

study of the vector distribution in tissues other than the liver revealed that the sole abolition of the CAR binding does not result in any modification of the transduction of the lung, heart, kidney, and spleen (Fig. 5 and Table 2). In contrast, the additional deletion of the RGD motif from the penton base caused a marked reduction in the level of vector genomes detected in the lung, heart, and kidney. These results corroborate those obtained by Einfeld *et al.* [26] and demonstrate the strong influence of the penton base interaction in most tissues apart from liver.

Two other groups [24,25] have reported liver transduction data inconsistent with those described by Einfeld *et al.* [26]. Smith *et al.* were unable to reproduce the effect on liver transduction of the R<sub>412</sub>AEK<sub>417</sub> → SGGG mutation [24] and suggested that this discrepancy could be related to polymorphism in the viral backbone or capsid. Another explanation for this observation could be that the specific mutations of the fiber and penton base used by Einfeld *et al.* may result in some unexpected and efficient uptake by specialized cells (such as macrophages) or organs in a CAR/integrin-independent manner, thus preventing the vector from efficiently infecting hepatocytes. Finally, as exemplified by Mizuguchi *et al.* with Ad vectors containing an RGD peptide in fiber HI loop [25], the systematic inclusion of the influenza HA epitope in the vector capsids may retarget the vectors to untargeted cells such as erythrocytes, thereby explaining the dramatic decrease in liver gene transfer.

Altogether, the evidence that the elimination of Ad5 binding to CAR alone, to  $\alpha_v$  integrins alone, or to both targets does not reduce Ad5 liver tropism implies that virus entry can occur *in vivo* independent of CAR and  $\alpha_v$  integrins. Some studies using chimeric vectors provide additional clues to understanding the Ad5 entry pathway in the liver. The subgroup B Ad3 and Ad35 serotypes are known to bind to a receptor distinct from CAR. Consistently, it has been reported that chimeric viruses containing the Ad3 or Ad35 knob fused to an Ad3 shaft (6 repeats long) or to an Ad5 shaft (22 repeats long) transduce cells *in vitro* in a CAR-independent fashion [34–36]. Yet *in vivo*, the long-shafted vector exhibits an intact hepatotropism, confirming that liver gene transfer occurs in a CAR-independent way [34–36]. In contrast, the short-shafted vectors demonstrated a 10-fold reduction in liver gene transfer. One explanation for the difference between liver transduction with short- and long-shafted vectors is that a short shaft may confer to the virion physical properties unsuitable for accessing hepatocytes. Liver vessels exhibit pores up to 100 nm in width, whereas the Ad5 virion has a diameter of 80 nm without the fibers [37]. As they can infect hepatocytes efficiently, Ad5-based vectors displaying long and flexible fibers should have a total diameter inferior to the size of the pores. Shortening the fiber shaft may result in relative shaft rigidity, providing the virion with a total diameter larger than the pore size and thus preventing it from escaping vasculature and accessing

hepatocytes. Alternatively, one possible role of the shaft could be to bind to cellular receptors such as heparan sulfate glycosaminoglycans, known to mediate Ad5 binding to primary mouse hepatocytes and other cells [24,38]. Accordingly, this hypothesis may account for the lack of impact of CAR-binding-ablating knob mutations on liver tropism of viruses displaying an intact Ad5 shaft and may explain the discrepancy between hepatotropism of short- and long-shafted vectors.

Overall, the results presented here combined with previous reports [21,24,25,27] highlight the gap between the *in vitro* two-step entry pathway accepted for Ad5 and the mechanisms by which Ad5-based vectors infect hepatocytes *in vivo*. The identification of all the parameters involved in liver transduction should be essential for the development of fully detargeted and ultimately retargeted vectors. When such vectors are available, the VN4 peptide may prove useful for subsequent systemic delivery to specific tissues.

## MATERIALS AND METHODS

**Cells.** Cell culture media were from Gibco (Gibco, Invitrogen Corp., Cergy-Pontoise, France) and fetal bovine serum (FBS) was from Hyclone (Logan, UT, USA).

The 293 cell line (CRL1573, American Type Culture Collection, Rockville, MD, USA) was grown in modified Eagle's medium (MEM) supplemented with 10% FBS. The W162 cell line [39] and the 911 cells (kindly provided by Dr. R. Hoeben, University of Leiden, The Netherlands) were maintained in Dulbecco MEM (DMEM) supplemented with 10% FBS. Rat primary hepatocytes were kindly provided by Dr. C. Gianini (Institut Pasteur–Necker, Paris, France) [40]. L929 murine fibrosarcoma cells were obtained from Dr. U. Greber (Institute of Molecular Biology, Zurich, Switzerland) and maintained in DMEM supplemented with 10% FBS.

**Adenoviral vector construction and production.** Ad-CTL virus is derived from Ad5 and deleted for both the E1 and the E3 regions [41]. All viruses were constructed using homologous recombinational cloning in *Escherichia coli* and have a CMV/LacZ expression cassette in place of the E1 genes [41]. All fiber modifications were obtained using standard molecular biology techniques. Plasmid adenoviral backbones pKM14, pKM16, and AE77c display the P409E, K417A, and  $\Delta$ TAYT knob mutations, respectively. AE43c and pKM17 plasmid backbones were derived from control AE18c and pKM16 by substitution of the G<sub>538</sub>TQETGDTTPS<sub>548</sub> residues from the HI fiber loop with the RGHSRGRNQNSR VN4 ligand flanked with GSS linkers [33]. AE74c, pKM22, and pKM25 backbones were obtained from AE18c, pKM16, and pKM17, respectively, by replacement of the penton base H<sub>337</sub>AIRGDTFAT<sub>346</sub> sequence with a threonine–serine motif. All plasmids were checked by restriction analysis and DNA sequencing. Following transfection of plasmid backbones in standard E1-transcomplementing cells (911 or 293 cells), the corresponding viruses were generated, amplified, and purified from cell lysates by two successive CsCl ultracentrifugation steps [42] and titrated by HPLC [43]. Typically, high-titer purified preparations of Ad-VN4, Ad-PB<sub>μ</sub>, Ad-K417A-VN4, and control Ad-CTL were obtained using standard procedures (m.o.i. of 100 VP/cell and harvest 3 days postinfection). In the cases of Ad-P409E, Ad-K417A, Ad-K417A-PB<sub>μ</sub>, and Ad- $\Delta$ TAYT viruses, infection was performed at an m.o.i. of 100 or 1000 VP/cell, and cells were harvested at complete cytopathic effect, i.e., 3 to 5 days following infection. All subsequent experiments were performed with at least two independent purified preparations of each virus, so that results presented in this paper are representative.

***In vitro* transduction experiments.** All the experiments were performed in 12-well dishes in duplicate. For 293 competition experiments, cell mono-

layers were preincubated 30 min at room temperature with 10 µg/ml of purified recombinant Ad5 knob (a kind gift from Dr. R. Gerard, University of Michigan, Ann Arbor, MI, USA) or phosphate-buffered saline (PBS), before addition of the virus at an m.o.i. of 50 VP/cell. Thirty minutes later, cells were washed twice with PBS and further incubated 24 h at 37°C with fresh medium. L929 cells and rat primary hepatocytes were infected at an m.o.i. of 10,000 and 100 VP/cell, respectively. After 1 h or 30 min incubation at 37°C, cells were washed twice with PBS and further incubated with fresh medium 24 to 48 h at 37°C.

β-Galactosidase activity of the whole-cell extracts was quantified in a chemiluminescence assay (Clontech, Palo Alto, CA, USA) according to the supplier's recommendations. Protein concentration was determined using the Bio-Rad Protein Assay with bovine serum albumin as standard.

**In vitro binding of modified viruses to soluble CAR.** Soluble CAR (0.5 or 0.05 µg; a kind gift from Dr. D. Curiel, University of Alabama, Birmingham, AL, USA) was immobilized onto a nitrocellulose membrane. After being blocked for 1 h in PBS–5% non-fat dry milk, membranes were incubated with 10<sup>9</sup> or 10<sup>10</sup> VP of virus in PBS–0.5% nonfat dry milk at 4°C overnight. After two washes in PBS–0.5% nonfat dry milk–0.05% Igepal CA-630 (Sigma, France), membranes were incubated with a 1/2000 dilution of the L5 antibody that recognizes the whole Ad5 virion, for 2 h at room temperature. Membranes were washed twice and incubated with a 1/100,000 dilution of goat anti-rabbit secondary antibody conjugated to horseradish peroxidase (Jackson ImmunoResearch Laboratories, West Grove, PA, USA). The blot was finally revealed using the ECL Western blot detection kit (Amersham-France, France) according to the supplier's recommendations.

**In vivo experiments.** Control or modified virus (3 × 10<sup>10</sup> VP) was injected in the retro-orbital plexus of 6- to 8-week-old female C57BL/6 mice (Janvier, Le Genest-St-Isle, France). Animals were sacrificed 2 days following injection and liver, heart, lung, kidney, and spleen were collected, frozen in liquid nitrogen, and kept at –80°C until analysis. Fifty milligrams of liver tissue were placed in lysing matrix tubes containing 1 ml of suitable buffer and homogenized via the FastPrep System (Bio 101, Vista, CA, USA). Resulting homogenates were clarified by centrifugation at 12,000 rpm for 10 min at 4°C. For protein extraction, the lysis buffer was 0.2% Triton X-100, 0.5 mM DTT, 100 mM potassium phosphate, and one Complete protease inhibitor cocktail tablet (Roche Diagnostics, Meylan, France) per 25 ml of buffer. After centrifugation, the supernatant was measured for β-galactosidase activity using a chemiluminescence assay (Clontech). Protein content was determined using the Bio-Rad Protein Assay.

For DNA extraction, the Promega Wizard Genomic DNA Purification Kit Nuclei Lysis Solution was used as lysis buffer. After centrifugation, total DNA was recovered according to the manufacturer's instructions. Absorbances at 260 and 280 nm were measured and after proper dilution 50 ng of genomic DNA was subjected to quantitative PCR in duplicate samples.

**Quantitative PCR.** A real-time PCR was performed using the ABI Prism 7700 system and buffers provided by the manufacturer (Perkin-Elmer Applied Biosystems, Foster City, CA, USA) with 50 ng of each sample. The primers (sense 5'-YCCCATGGAYGAGCCACMCT-3' and antisense 5'-GAGAASGGBGTGCGCAGGTASAS-3') and the fluorogenic probe (5'-CAC-CAGCCACACCGCGCGTCATCGA-3') are located in the hexon gene (Y = C or T, M = A or C, S = G or C, and B = C or G or T) (P. Saulnier *et al.*, manuscript in preparation). The probe was linked at its 5' terminus with a reporter dye (6-carboxyfluorescein) and with a quencher dye (6-carboxy-N,N,N',N'-tetramethylrhodamine) at its 3' end. One microgram of human and murine genomic DNA (Roche Molecular Biochemicals, Meylan, France) was used to show the specificity of the Ad5 PCR. Samples were submitted to 50 PCR cycles with continuous monitoring of the fluorescence.

**Statistical analysis.** All *in vivo* data are shown as means ± standard error of the mean. Statistical analysis was performed using unpaired *t* test with Welch. Threshold for significance was set to *P* = 0.05.

## ACKNOWLEDGMENTS

We thank Pierre Boulanger (Université Claude Bernard, Lyon, France), Karim Benihoud (UMR 1582, Institut Gustave Roussy, France), Jean-François Dedieu (Gencell S.A., S., France), and Martine Latta-Mahieu (Aventis Pharma, France) for their constant interest and critical reading of the manuscript; Chantal Carrez (Aventis Pharma, France) for helpful advice in knob mutation design; Paule Opolon (UMR 1582, Institut Gustave Roussy, France) and Elisabeth Comault (UMR 1582, Institut Gustave Roussy, France) for their constant assistance with the *in vivo* studies; Stéphanie Esselin (UMR 1582, Institut Gustave Roussy, France) for technical assistance; and the entire staff of the animal facility at Institut Gustave Roussy. K.M. was supported by the Ministère de la Recherche et la Technologie (MRT) and the Association pour la Recherche contre le Cancer (ARC).

RECEIVED FOR PUBLICATION OCTOBER 22, 2002; ACCEPTED MAY 18, 2003.

## REFERENCES

- Wickham, T. J. (2000). Targeting adenovirus. *Gene Ther.* 7: 110–114.
- Preissner, K. T., Kanse, S. M., and May, A. E. (2000). Urokinase receptor: A molecular organizer in cellular communication. *Curr. Opin. Cell Biol.* 12: 621–628.
- Reuning, U., *et al.* (1998). Multifunctional potential of the plasminogen activation system in tumor invasion and metastasis. *Int. J. Oncol.* 13: 893–906.
- Nakata, S., *et al.* (1998). Involvement of vascular endothelial growth factor and urokinase-type plasminogen activator receptor in microvessel invasion in human colorectal cancers. *Int. J. Cancer* 79: 179–186 doi:10.1002/(sci)10976-0215(19980417):79:2:179.
- Hildenbrand, R., *et al.* (1998). Urokinase receptor localization in breast cancer and benign lesions assessed by *in situ* hybridization and immunohistochemistry. *Histochem. Cell Biol.* 110: 27–32.
- Bergelson, J. M., *et al.* (1997). Isolation of a common receptor for coxsackie B viruses and adenoviruses 2 and 5. *Science* 275: 1320–1323.
- Tomko, R. P., Xu, R., and Philipson, L. (1997). HCAR and MCAR: The human and mouse cellular receptors for subgroup C adenoviruses and group B coxsackieviruses. *Proc. Natl. Acad. Sci. USA* 94: 3352–3356.
- Wickham, T. J., *et al.* (1993). Integrins alpha v beta 3 and alpha v beta 5 promote adenovirus internalization but not virus attachment. *Cell* 73: 309–319.
- Mathias, P., Galleno, M., and Nemerow, G. R. (1998). Interactions of soluble recombinant integrin alpha v beta 5 with human adenoviruses. *J. Virol.* 72: 8669–8675.
- Chiu, C. Y., *et al.* (1999). Structure of adenovirus complexed with its internalization receptor, alphavbeta5 integrin. *J. Virol.* 73: 6759–6768.
- Walters, R. W., *et al.* (1999). Basolateral localization of fiber receptors limits adenovirus infection from the apical surface of airway epithelia. *J. Biol. Chem.* 274: 10219–10226.
- McDonald, D., *et al.* (1999). Coxsackie and adenovirus receptor (CAR)-dependent and major histocompatibility complex (MHC) class I-independent uptake of recombinant adenoviruses into human tumour cells. *Gene Ther.* 6: 1512–1519.
- Hutchin, M. E., Pickles, R. J., and Yarbrough, W. G. (2000). Efficiency of adenovirus-mediated gene transfer to oropharyngeal epithelial cells correlates with cellular differentiation and human coxsackie and adenovirus receptor expression. *Hum. Gene Ther.* 11: 2365–2375.
- Hemmi, S., *et al.* (1998). The presence of human coxsackievirus and adenovirus receptor is associated with efficient adenovirus-mediated transgene expression in human melanoma cell cultures. *Hum. Gene Ther.* 9: 2363–2373.
- Kasono, K., *et al.* (1999). Selective gene delivery to head and neck cancer cells via an integrin targeted adenoviral vector. *Clin. Cancer Res.* 5: 2571–2579.
- Douglas, J. T., *et al.* (2001). Efficient oncolysis by a replicating adenovirus (ad) in vivo is critically dependent on tumor expression of primary ad receptors. *Cancer Res.* 61: 813–817.
- Bewley, M. C., *et al.* (1999). Structural analysis of the mechanism of adenovirus binding to its human cellular receptor, CAR. *Science* 286: 1579–1583.
- Roelvink, P. W., *et al.* (1999). Identification of a conserved receptor-binding site on the fiber proteins of CAR-recognizing adenoviridae. *Science* 286: 1568–1571.
- Kirby, I., *et al.* (1999). Mutations in the DG loop of adenovirus type 5 fiber knob protein abolish high-affinity binding to its cellular receptor CAR. *J. Virol.* 73: 9508–9514.
- Jakubczak, J. L., *et al.* (2001). Adenovirus type 5 viral particles pseudotyped with mutagenized fiber proteins show diminished infectivity of coxsackie B-adenovirus receptor-bearing cells. *J. Virol.* 75: 2972–2981 doi:10.1128/jvi.75.6.2972-2981.2001..
- Leissner, P., *et al.* (2001). Influence of adenoviral fiber mutations on viral encapsidation, infectivity and *in vivo* tropism. *Gene Ther.* 8: 49–57.
- Nicklin, S. A., *et al.* (2001). Ablating adenovirus type 5 fiber-CAR binding and HI loop insertion of the SIGYPLP peptide generate an endothelial cell-selective adenovirus. *Mol. Ther.* 4: 534–542 doi:10.1006/mthe.2001.0489..
- Cripe, T. P., *et al.* (2001). Fiber knob modifications overcome low, heterogeneous

- expression of the coxsackievirus-adenovirus receptor that limits adenovirus gene transfer and oncolysis for human rhabdomyosarcoma cells. *Cancer Res.* **61**: 2953–2960.
24. Smith, T., *et al.* (2002). In vivo hepatic adenoviral gene delivery occurs independently of the coxsackievirus-adenovirus receptor. *Mol. Ther.* **5**: 770–779.
  25. Mizuguchi, H., *et al.* (2002). CAR- or alpha v integrin-binding ablated adenovirus vectors, but not fiber-modified vectors containing RGD peptide, do not change the systemic gene transfer properties in mice. *Gene Ther.* **9**: 769–776.
  26. Einfeld, D. A., *et al.* (2001). Reducing the native tropism of adenovirus vectors requires removal of both CAR and integrin interactions. *J. Virol.* **75**: 11284–11291.
  27. Alemany, R., and Curiel, D. T. (2001). CAR-binding ablation does not change biodistribution and toxicity of adenoviral vectors. *Gene Ther.* **8**: 1347–1353.
  28. Fechner, H., *et al.* (1999). Expression of coxsackie adenovirus receptor and alphav-integrin does not correlate with adenovector targeting in vivo indicating anatomical vector barriers. *Gene Ther.* **6**: 1520–1535.
  29. Huard, J., *et al.* (1995). The route of administration is a major determinant of the transduction efficiency of rat tissues by adenoviral recombinants. *Gene Ther.* **2**: 107–115.
  30. Katagiri, Y. U., *et al.* (1996). Non-RGD domains of osteopontin promote cell adhesion without involving alpha v integrins. *J. Cell. Biochem.* **62**: 123–131.
  31. Solberg, H., *et al.* (2001). The murine receptor for urokinase-type plasminogen activator is primarily expressed in tissues actively undergoing remodeling. *J. Histochem. Cytochem.* **49**: 237–246.
  32. Kirby, I., *et al.* (2000). Identification of contact residues and definition of the CAR-binding site of adenovirus type 5 fiber protein. *J. Virol.* **74**: 2804–2813.
  33. Waltz, D. A., *et al.* (1997). Plasmin and plasminogen activator inhibitor type 1 promote cellular motility by regulating the interaction between the urokinase receptor and vitronectin. *J. Clin. Invest.* **100**: 58–67.
  34. Kanerva, A., *et al.* (2002). Gene transfer to ovarian cancer versus normal tissues with fiber-modified adenoviruses. *Mol. Ther.* **5**: 695–704 doi:10.1006/mthe.2002.0609..
  35. Vigne, E., *et al.* (2003). Genetic manipulation of adenovirus type 5 fiber resulting in liver tropism attenuation. *Gene Ther.* **10**: 153–162.
  36. Shayakhmetov, D. M., *et al.* (2002). Targeting of adenovirus vectors to tumor cells does not enable efficient transduction of breast cancer metastases. *Cancer Res.* **62**: 1063–1068.
  37. Ruigrok, R. W., *et al.* (1990). Structure of adenovirus fibre. II. Morphology of single fibres. *J. Mol. Biol.* **215**: 589–596.
  38. Dehecchi, M. C., *et al.* (2001). Heparan sulfate glycosaminoglycans are receptors sufficient to mediate the initial binding of adenovirus types 2 and 5. *J. Virol.* **75**: 8772–8780.
  39. Weinberg, D. H., and Ketner, G. (1983). A cell line that supports the growth of a defective early region 4 deletion mutant of human adenovirus type 2. *Proc. Natl. Acad. Sci. USA* **80**: 5383–5386.
  40. McIntyre, M., *et al.* (1999). Differential expression of the cyclin-dependent kinase inhibitor P27 in primary hepatocytes in early-mid G1 and G1/S transitions. *Oncogene* **18**: 4577–4585.
  41. Crouzet, J., *et al.* (1997). Recombinational construction in *Escherichia coli* of infectious adenoviral genomes. *Proc. Natl. Acad. Sci. USA* **94**: 1414–1419.
  42. Graham, F. L., and Prevec, L. (1995). Methods for construction of adenovirus vectors. *Mol. Biotechnol.* **3**: 207–220.
  43. Blanche, F., *et al.* (2000). An improved anion-exchange HPLC method for the detection and purification of adenoviral particles. *Gene Ther.* **7**: 1055–1062.
  44. Xia, D., Henry, L. J., Gerard, R. D., and Deisenhofer, J. (1994). Crystal structure of the receptor-binding domain of adenovirus type 5 fiber protein at 1.7 Å resolution. *Structure* **2**: 1259–1270.